Performance Analysis of the Interferometric Ranging System with Hopped Frequencies against Multi-tone Jammer

Yue Zhang and Wangdong Qi*
Center of Network Engineering, PLA University of Science and Technology, Nanjing, 210007, China
Email: {zhyemf, wangdongqi}@gmail.com

***Abstract*—Interferometric Ranging System with Hopped Frequencies (IRHF) is a novel ranging technique with advanced anti-jamming capability in wireless sensor networks. This paper investigates the ranging performance of Maximum Likelihood (ML) estimator of IRHF under multi-tone jamming (MTJ), which is a potential threat faced by wireless sensor nodes. Firstly, the jamming model with one malicious node transmitting MTJ signal is introduced. Secondly, the region where the false estimation locates is detected. Finally, a closed-form expression of the probability of false estimation versus signal-to-jamming ratio and some system parameters is derived with the tool of pair-wise probability. The consistence between the simulation results and the theoretical approximations validates our analyses. The study shows that the probability of false estimation proposed here can predict the ML ranging performance of IRHF accurately and relieve the requirement of time-consuming computer simulations.**

***Index Terms*—Interferometric ranging system with hopped frequencies, multi-tone jamming, maximum likelihood estimator, probability of false estimation, pair-wise probability**

I. Introduction

Localization plays an important role in the applications of Wireless Sensor Networks (WSN) [1]-[3]. The traditional range-based schemes, implemented by measuring TOA (Time of Arrival), TDOA (Time Difference on Arrival) and AOA (Angle of Arrival), provide high accuracy but are difficult to implement in the low-cost and energy-constrained wireless sensor nodes. The techniques based on received signal strength indicator (RSSI) require no extra devices but result in low accuracy [4]. In contrast, the Radio Interferometric Positioning System (RIPS), a novel range-based method proposed in the year of 2005, achieves high accuracy with simple and low-cost hardware. The prototype implementation on the MICA2 platform achieves an average error of 4 cm covering an 120× 120 m area [5]-[8].

Manuscript received January 1, 2014; revised February 1, 2014; accepted April 1, 2014.
*Corresponding author

The critical technique employed in RIPS is the Radio Interferometric Ranging (RIR), which has received considerable attention recently. In range measurement, Zhu extends the deployment area to over one kilometers by optimizing parameters [9], and Qi proposes two-frequency-interval method to keep comparable localization accuracy with large range [10], meanwhile, Wang and Xu calculates the distance directly from closed-form equation based on Extended Chinese Remainder Theorem (ECRT) [11][12]. In order to mitigate multipath, Ledeczi proposes a one-dimensional indoor tracking approach [13], and Liu employs multiple carrier frequencies from large enough bandwidth to measure ground surface displacement for landslide early warning [14]. Except for the successful applications in asynchronous positioning system by transmitting two slightly different dual-tone signals [15], some researchers also investigate how to improve the estimator's efficiency [16], increase the localization accuracy [17], extend the deployment [18] and analyze the ranging performance [19].

All the achievements above focus on the civil applications in benign environment, where the measurement frequencies of RIPS involves stepped frequencies with uniform space. It deserves considerable attention that RIPS has potential to serve sensor nodes in military scenario. Weili has extended the usages of RIPS by introducing frequency hopping spread spectrum (HFSS) [20], and we call it Interferometric Ranging Systems with Hopped Frequencies (IRHF). IRHF is well suited for military applications, especially when the nodes are deployed in hostile environment to track entities, monitor environment or perform battlefield surveillance [21]-[23].

In these military scenarios, sensor nodes may suffer from severe interference. These interferences can be categorized into two types [24]-[26]: in the monitor area with dense sensor nodes, the frequency bands of different radio signals may interference with each other without intention, which is unintentional interference. In the battlefield, the malicious nodes may emit jamming signals to weaken the strength of received signal or alter the information intend to be received, which is intentional jamming. This paper considers the latter one.

doi:10.4304/jcp.9.9.2222-2229

For the FHSS systems, partial band noise jamming (PBNJ) and multi-tone jamming (MTJ) are two of the most effective jamming signals. Literature [27] has investigated the ranging performance of IRHF under PBNJ environment, implying that the worst-case jamming is full-band jamming. In this paper, we focus on the ranging performance of IRHF against MTJ.

Theoretical analysis in this paper shows that the decreased performance of IRHF caused by MTJ reflects on the false estimation of distance. It seems like that the malicious node takes place of the ranging node and produces a mistaken distance. Taking this effect into account, we believe that it is not sufficient to understand the ranging performance through the mean square error (MSE). Therefore we pay attention to the probability of false estimations caused by attacker nodes. A closed-form expression is derived about this probability versus signal-to-jamming ratio (SJR) and some system parameters, which is verified by simulation results. This paper provides a theoretical tool in describing the performance of IRHF under multi-tone jamming.

The rest of this paper is organized as follows. The system model of IRHF and the jamming model are presented in section 2. Section 3 shows the false distance estimation under multi-tone jamming. The probability of false estimations is calculated in section 4. Section 5 gives the simulation results and the discussions. We make a few conclusions in Section 6.

II. System Model

A. Model of IRHF

The structure of IRHF that based on RIPS is shown in Fig.1. The IRHF requires two nodes, A and B, to transmit sine waves at two close frequencies f_A and f_B simultaneously, resulting in an interference signal with envelope frequency $\delta = | f_A - f_B |$. Two receivers C and D measure the phase of the interference signal respectively. These four nodes have composed a ranging unit. The relative phase offset between C and D is a function of the linear combination of distances between the four nodes A, B, C and D [5].

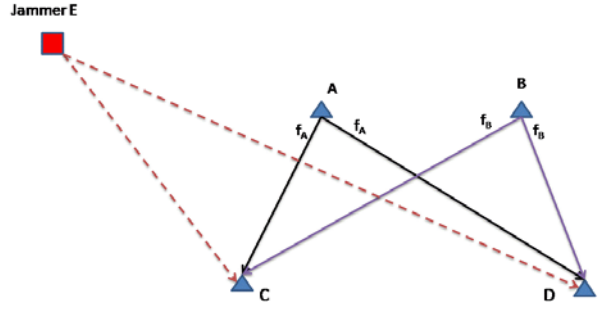

Figure 1. IRHF principle diagram (the triangles represent normal ranging nodes and the rectangular represents malicious node).

In fact, by demodulating the signal into baseband, one can complete the phase estimation process with low-cost hardware [18]. Because this method is suitable to implement in software-defined radio platform with high quality, the following analysis will be carried out based on demodulation method.

In the absence of noise, the received signals of node C and D have the complex forms that

$$r_C(t) = a_{AC} \exp\left(j2\pi f_A (t - \frac{d_{AC}}{c}) + j\phi_A \right) + a_{BC} \exp\left(j2\pi f_B (t - \frac{d_{BC}}{c}) + j\phi_B \right) \quad (1)$$

$$r_D(t) = a_{AD} \exp\left(j2\pi f_A (t - \frac{d_{AD}}{c}) + j\phi_A \right) + a_{BD} \exp\left(j2\pi f_B (t - \frac{d_{BD}}{c}) + j\phi_B \right) \quad (2)$$

Where c is the speed of light, d_{XY} is the distance from node X to node Y, a_{XY} is the signal amplitude of signal from node X at node Y. The phases ϕ_A and ϕ_B , uniformly distributed in the interval $(-\pi, \pi)$, are random variables including the time synchronization errors. As for nodes C and D, The phase offsets of the signals from A and B is

$$\phi_C = \phi_{AC} - \phi_{BC} = \frac{2\pi}{c}(f_B d_{BC} - f_A d_{AC}) + (\phi_A - \phi_B) \mod 2\pi \quad (3)$$

$$\phi_D = \phi_{AD} - \phi_{BD} = \frac{2\pi}{c}(f_B d_{BD} - f_A d_{AD}) + (\phi_A - \phi_B) \mod 2\pi \quad (4)$$

And the difference between ϕ_C and ϕ_D is

$$\phi = \phi_C - \phi_D = (\phi_{AC} - \phi_{BC}) - (\phi_{AD} - \phi_{BD}) \quad (5)$$

According to the *theorem* 3 in literature [5], the phase offset ϕ is unrelated to the random variables ϕ_A or ϕ_B and has a clear relationship with the distance to be estimated:

$$\phi \approx \frac{2\pi f}{c} d_0 \quad (6)$$

where $f = (f_A + f_B)/2$ is the carrier frequency and $d_0 = d_{AD} - d_{AC} + d_{BC} - d_{BD}$ is a linear combination of distances between the four nodes A, B, C and D.

After getting a set of the combined phases from a series of measurements with multiple carrier frequencies, we have the observations that

$$\phi_i = \frac{2\pi f_i}{c} d_0 \ (\mathrm{mod} 2\pi), i = i, \cdots, M \quad (7)$$

Where M is the number of the carrier frequencies. It is assumed that all carrier frequencies f_i are chosen randomly within the bandwidth W_{ss}. They are multiples of the system's minimum frequency interval f_{min} that $f_i = (k_0 + k_i) f_{min}$, where $k_0 f_{min}$ is the initial frequency and $k_i f_{min}$ denotes the frequency step. The number of maximum chosen frequencies is $N = W_{ss} / f_{min} + 1$. the positive integer k_i distributes uniformly within $[0, N-1]$.

At moderate/high signal-to-noise ratio (SNR), the equations (7) can be converted into the equivalent form that

$$\exp(j\phi_i) = \exp\left(j\frac{2\pi f_i}{c} d_0 \right) \tag{8}$$

Some routine computations give rise to the ML estimator of d_0 by maximizing the criterion function

$$F(d) = \left| \sum_{i=1}^{M} \left\{ \exp(j\phi_i) \exp(-j2\pi \frac{f_i}{c} d) \right\} \right| \tag{9}$$

If we have the knowledge of the locations of three out of four nodes, for example A, B and C, then both distances d_{AC} and d_{BC} are known and the estimated distance of d_0 defines a hyperboloid with foci C and D. It is easy to see that the location of D can be found at intersection of several hyperboloids defined by these distances d_0 [7]. This paper considers only the ranging performance of IRHF, while its localization performance under multi-tone jamming is to be discussed in our future work.

B. Model of Multi-Tone Jammer

In the environment of jamming, we assume that node E locates near the ranging unit and transmits MTJ signals, as seen in Fig. 1. We call this node E a '*malicious node*'. It is seen that interfering one of the transmitters is sufficiently to destroy the distance information. Without loss of generality, we assume that the aim of this malicious node is to interference node A. We also assume that the possible locations of the hopped frequencies of node A are known by E, even though the hop sequence is not [25].

As an intelligent jammer, E splits the total available jamming power among Q sine wave tones with random phase. The fraction of the channels been jammed is $\beta = Q/N$, so the measurement frequency will be jammed with the probability β and not jammed with the probability $1-\beta$.

In general, The distance from E to C is different from the distance from E to D, resulting in different signal strengths at the two receivers. Take the node C for example, the equivalent spectrum density among the bandwidth W_{ss} of the jammer power is denoted by I_c. Consequently the jamming signal received by C in f_A is represented in the complex form by

$$r'_C(t) = \sqrt{J_c} \exp\left(j2\pi f_A (t - \frac{d_{EC}}{c}) + j\phi_E \right) \tag{10}$$

where $J_c = I_c N / Q = I_c / \beta$. For comparison we denote the power spectrum of signal received by C from A is S_c, and $a_{AC} = \sqrt{S_c}$, so the SJR at node C is S_c / I_c .

Similarly, the jamming signal received by node D in f_B has the form

$$r'_D(t) = \sqrt{J_d} \exp\left(j2\pi f_B (t - \frac{d_{ED}}{c}) + j\phi_E \right) \tag{11}$$

where $J_d = I_d / \beta$ and I_d is the equivalent spectrum density of jammer signal. If S_d denotes the power spectrum of signal received by D from A, then the SJR at node D is S_d / I_d with $a_{AD} = \sqrt{S_d}$. In ordinary conditions, we have $S_c / I_c \neq S_d / I_d$.

III. False Estimation Caused by Multi-Tone Jamming

In this section, we will explore the ill-effect caused by multi-tone jamming with the model in the previous section. Note that the phases ϕ_{AC} and ϕ_{AD} will be contaminated if the signal transmitted from A is jammed. We denote the contaminated phases are ϕ'_{AC} and ϕ'_{AD} , then

$$\begin{aligned} \phi'_{AC} = \arg\Big\{ & \sqrt{S_c} \exp\left(j2\pi f_A (t - \frac{d_{AC}}{c}) + j\phi_A \right) \\ & + \sqrt{J_c} \exp\left(j2\pi f_A (t - \frac{d_{EC}}{c}) + j\phi_E \right) \Big\} \end{aligned} \tag{12}$$

$$\begin{aligned} \phi'_{AD} = \arg\Big\{ & \sqrt{S_d} \exp\left(j2\pi f_A (t - \frac{d_{AD}}{c}) + j\phi_A \right) \\ & + \sqrt{J_d} \exp\left(j2\pi f_A (t - \frac{d_{ED}}{c}) + j\phi_E \right) \Big\} \end{aligned} \tag{13}$$

As a result, the contaminated phase information involved in estimating distance under MTJ is denoted by

$$\phi' = (\phi'_{AC} - \phi_{BC}) - (\phi'_{AD} - \phi_{BD}) \tag{14}$$

It is obvious that the contaminated phases ϕ' are not equal to the original one of ϕ in (5), leading to a false estimation of the distance.

Being aware of the exact values of ϕ'_{AC} and ϕ'_{AD} will give rise to the information where the false estimator is located, however it is complicated to calculate them from equation (12) and (13). We note that all the phases used to estimate distance in (9) are within the manipulation of $\exp(\cdot)$, so in the following we focus on the values of $\exp(j\phi'_{AC})$ and $\exp(j\phi'_{AD})$ instead of the exact value of ϕ'_{AC} and ϕ'_{AD} .

It is not difficult to obtain that

$$\begin{aligned} \exp(j\phi'_{AC}) = \; & a_{sc} \exp\left(j2\pi f_A (t - \frac{d_{AC}}{c}) + j\phi_A \right) \\ & + a_{Jc} \exp\left(j2\pi f_A (t - \frac{d_{EC}}{c}) + j\phi_E \right) \end{aligned} \tag{15}$$

$$\begin{aligned} \exp(j\phi'_{AD}) = \; & a_{sd} \exp\left(j2\pi f_A (t - \frac{d_{AD}}{c}) + j\phi_A \right) \\ & + a_{Jd} \exp\left(j2\pi f_A (t - \frac{d_{ED}}{c}) + j\phi_E \right) \end{aligned} \tag{16}$$

where $a_{sc} / a_{Jc} = \sqrt{S_c / J_c}$, $a_{sd} / a_{Jd} = \sqrt{S_d / J_d}$ and $\sqrt{a_{sc}^2 + a_{Jc}^2} = \sqrt{a_{sd}^2 + a_{Jd}^2} = 1$. According to the manipulation in (14), we have

$$\exp(j\phi'_{AC})\exp(-j\phi'_{AD}) = a_{Jc}a_{Jd}\exp\left(\frac{j2\pi f_A}{c}(d_{ED}-d_{EC})\right) + a_{sc}a_{sd}\exp\left(\frac{j2\pi f_A}{c}(d_{AD}-d_{AC})\right)+n \quad (17)$$

where

$$n = a_{Jc}a_{sd}\exp\left(\frac{j2\pi f_A}{c}(d_{AD}-d_{EC})-j(\phi_A-\phi_E)\right) + a_{sc}a_{Jd}\exp\left(\frac{j2\pi f_A}{c}(d_{ED}-d_{AC})+j(\phi_A-\phi_E)\right) \quad (18)$$

Because ϕ_A and ϕ_E are random variables, we regard n as random noise without effective information. On the other hand, the signals transmitted from B are not jammed and the phases of the signals from B at the receivers C and D are

$$\exp(j\phi_{BC}) = \exp\left(j2\pi f_B(t-\frac{d_{BC}}{c})+j\phi_B\right) \quad (19)$$

$$\exp(j\phi_{BD}) = \exp\left(j2\pi f_B(t-\frac{d_{BD}}{c})+j\phi_B\right) \quad (20)$$

Combining the *theorem* 3 in [5] with the equations (15) to (20), we have

$$\exp(j\phi') \approx a_s\exp\left(j\frac{2\pi f}{c}d_0\right)+a_J\exp\left(j\frac{2\pi f}{c}d'_0\right) \quad (21)$$

where $a_s = a_{sc}a_{sd}$, $a_J = a_{Jc}a_{Jd}$, $d_0 = d_{AD}-d_{AC}+d_{BC}-d_{BD}$, and $d'_0 = d_{ED}-d_{EC}+d_{BC}-d_{BD}$.

Comparing equations (8) and (21), we know that except for the true distance d_0 , the phase ϕ' contains the information corresponding to a false distance d'_0 . The coefficients a_s and a_J can be regarded as two different weights contributing to true value and false value of distance respectively.

It is also notable that the value d'_0 is a combination of four nodes E, B, C and D. This indicates that the malicious node E may replace the original node A, resulting in a false range estimation.

In the next section, we will explore how the malicious node would influence the ranging performance under different jamming parameters.

IV. Ranging Performance under Multi-Tone Jamming

IRHF belongs to the phase-based ranging technique. It is a straightforward way to assess the ranging performance of a phase-based ranging system in terms of MSE. Under MTJ environment, however, the analysis in the former section implies that the estimated distance of IRHF situates either at the true value or at the false one. As a result, the estimation error always maintains large value however the SJR is, so the MSE is not fit for the reflection of the degree of contamination caused by multi-tone jammer. It is necessary to propose a suitable indicator to assess the ranging performance against MTJ.

As we know, the anti-jamming capability is well studied in the field of digital communications. The 'bit-error probability' plays an important role to evaluate the reliability of communication systems [25]. Fortunately, we find that the false-estimation probability is similar to the bit-error probability in evaluating the reliability of ranging systems under jamming environment. So we plan to describe the anti-jamming capability of IRHF resorting to the false-estimation probability of range estimation against multi-tone jammer.

It is reasonable to assume that the system don't realize whether the measurement frequencies are jammed or not, and substitute all of phases back to (9) to estimate distance. Combining the results in former sections, we have the ML estimator of the distance d_0 under MTJ environment that by maximizing the criterion function

$$V(d) = \left|\sum_{i=1}^{M}\left\{\overline{p}_{i,l}\exp(j\phi_i)\exp(-j2\pi\tfrac{f_i}{c}d) + p_{i,l}\exp(j\phi'_i)\exp(-j2\pi\tfrac{f_i}{c}d)\right\}\right| \quad (22)$$

where $p_{i,0}=0, p_{i,1}=1$ and $\overline{p}_{i,l}=1-p_{i,l}$. The coefficients $p_{i,l}$ and $\overline{p}_{i,l}$ are the indicators whether the frequency f_i is jammed or not. We know that the probability $Pr\{p_{i,l}=p_{i,1}\}=\beta$ because the frequency f_i is jammed with probability β .

The probability of false estimation of d_0 depends on the value of $V(d)$ at different ranges of d. the analysis in the former section indicates that the most probable values of $\hat{d}_0$ locate at d_0 or d'_0 . So the probability of false estimations is

$$P = Pr[V(d_0) < V(d'_0)] \quad (23)$$

Let

$$y_0 = \sum_{i=1}^{M} y_{0i} = \sum_{i=1}^{M}\left\{\overline{p}_{i,l}+p_{i,l}(a_{si}+a_{Ji}r_i)\right\} \quad (24)$$

$$y_e = \sum_{i=1}^{M} y_{ei} = \sum_{i=1}^{M}\left\{\overline{p}_{i,l}r_i+p_{i,l}(a_{si}r_i+a_{Ji})\right\} \quad (25)$$

where $r_i = \exp(j2\pi\frac{f_i}{c}\Delta)$ and $\Delta = |d_0-d'_0|$. We denote that a_{si} and a_{Ji} has the same expressions as a_s and a_J in (21) correspondence to the ith frequency f_i. According to (23) we have $V(d_0)=|y_0|$, $V(d_e)=|y_e|$. Then the false-estimation probability can be expressed as

$$P = Pr(|y_0|<|y_e|) = Pr(|y_0|^2-|y_e|^2<0) \quad (26)$$

Because the coefficient of the $\exp(j\phi'_i)$ is 1, we have

$$a_{si} = \frac{\sqrt{S_cS_d}}{\sqrt{S_cS_d+J_cJ_d+2\sqrt{S_dS_dJ_cJ_d}\cos\left(\frac{2\pi f_i}{c}(\Delta)\right)}} \quad (27)$$

$$a_{Ji} = \frac{\sqrt{J_cJ_d}}{\sqrt{S_cS_d+J_cJ_d+2\sqrt{S_cS_dJ_cJ_d}\cos\left(\frac{2\pi f_i}{c}(\Delta)\right)}} \quad (28)$$

Computing the probability P depends on the distribution of y_0 and y_e , of which the calculation is quite involved. It is observed that y_0 as well as y_e , is the

summation of M independent identical distribution (i.i.d) random variables. In view of central-limit theorem, it is quite enough to guarantee that both y_0 and y_e are approximately Gaussian distributed if $M \geq 30$ [28], and the number M in IRHF always meets the requirement.

We note that the probability P is also called 'pair-wise probability ', which is a common concept related to the bit-error probability in the field of digital signal communications.

Combining the statement above and the condition that y_0 and y_e are correlated, we will get the expression of P resorting to *appendix B* in [29]. The effort is to calculate the means and second-order moments of y_0 and y_e, among of which the means and variances are M multiples of the means and variances of y_{0i} and y_{ei}.

We know that y_{0i} and y_{ei} are both mixture distributed. A nice feature of the mixture distribution is that the moments are quite easily available. Some manipulations based on the moments of mixture distribution [30] give that

$$\begin{aligned} E[y_{0i}] &= (1-\beta)+\beta\cdot m_1 \\ E[y_{ei}] &= (1-\beta)\cdot m_r+\beta\cdot m_2 \\ D[y_{0i}] &= (1-\beta)+\beta(m_1^2+v_1)-E[y_{0i}] \\ D[y_{ei}] &= (1-\beta)\cdot m_r^2+v_r)+\beta(m_2^2+v_2)-E[y_{ei}] \end{aligned} \tag{29}$$

where $m_1=\sum_{j=1}^{N}\frac{1}{N}(a_{sj}+a_{Jj}r_j)$, $m_2=\sum_{j=1}^{N}(a_{sj}r_j+a_{Jj})$,

$v_1=\sum_{j=1}^{N}\frac{1}{N}(a_{sj}+a_{Jj}r_j-m_1)^2$, $v_2=\sum_{j=1}^{N}(a_{sj}r_j+a_{Jj}-m_2)^2$,

$m_r=\sum_{j=1}^{N}\frac{r_j}{N}$, and $v_r=\sum_{j=1}^{N}(\frac{r_j}{N}-mr_j)^2$.

Because y_{0i} and y_{ei} are i.i.d random variables, the simple summations lead to the means of y_0 and y_e that

$$\begin{aligned} \overline{x} &= E[y_0]=M\cdot E[y_{0i}] \\ \overline{y} &= E[y_e]=M\cdot E[y_{ei}] \end{aligned} \tag{30}$$

and the second-order moments of y_0 and y_e that

$$\begin{aligned} \mu_{xx} &= D[y_0]=M\cdot D[y_{0i}] \\ \mu_{yy} &= D[y_e]=M\cdot D[y_{ei}] \\ \mu_{xy} &= cov[y_0,y_e]=M(1-\beta)\cdot m_r^* \\ &\quad + M\beta[m_{12}+(M-1)m_1\cdot m_2^*]-E[y_0]E[y_e]^* \end{aligned} \tag{31}$$

Where $m_{12}=\sum_{j=1}^{N}\left[\frac{1}{N}(a_{sj}+a_{Jj}r_j)(a_{sj}r_j+a_{Jj})^*\right]$.

Substituting formulas (30) and (31) into formula B-21 of [29], we have the closed-form expression of the probability of false estimation that

$$P=Q_1(a,b)-\frac{v_2/v_1}{1+v_2/v_1}\cdot I_0(ab)\exp[-\tfrac{1}{2}(a^2+b^2)] \tag{32}$$

where

$$a=\left[\frac{2v_1^2v_2(\alpha_1v_2-\alpha_2)}{(v_1+v_2)^2}\right]^{1/2} \quad , \quad b=\left[\frac{2v_1v_2^2(\alpha_1v_1+\alpha_2)}{(v_1+v_2)^2}\right]^{1/2} .$$

The items in a and b are as follow:

$$v_1=\sqrt{w^2+\frac{1}{4\left(\mu_{xx}\mu_{yy}-|\mu_{xy}|^2\right)}}-w \ ,$$

$$v_2=\sqrt{w^2+\frac{1}{4\left(\mu_{xx}\mu_{yy}-|\mu_{xy}|^2\right)}}+w \ ,$$

$$w=\frac{\mu_{xx}-\mu_{yy}}{4\left(\mu_{xx}\mu_{yy}-|\mu_{xy}|^2\right)} \ ,$$

$$\alpha_1=2\left(|\overline{x}|^2\mu_{yy}+|\overline{y}|^2\mu_{xx}-\overline{x}^*\overline{y}\mu_{xy}-\overline{xy}^*\mu_{xy}^*\right) \ ,$$

$$\alpha_2=|\overline{x}|^2-|\overline{y}|^2 \ .$$

The equation (32) depends on only four system parameters: the number of measurement frequencies M, the bandwidth W_{ss}, and the SJR at two receivers.

It is notable that the approximation of (27) and (28) are valid under the condition that the difference of SJRs at two nodes C and D is not large, which always meets the reality in practice.

V. Simulation Results

Some results of Monte Carlo simulations will now be presented in order to illustrate the accuracy of the analysis in the previous sections. The deployment of the sensor nodes is shown in Fig. 2. The triangle nodes A, B, locate at (2, 10) and (30, 16) representing transmitters, the circle ones C, D locate at (10, 0) and (24, 0) representing receivers, and the rectangular one locates at (20, 20) representing malicious node. It is easy to obtain the distances between the four nodes A, B, C and D that $d_{AD}=30.59$, $d_{BD}=17.09$, $d_{AC}=14.14$, $d_{BC}=25.61$. The distances between malicious node E and the receivers are $d_{EC}=22.36$, $d_{ED}=20.40$. Therefore, we get that $d_0=24.98$ and $d'_0=6.56$.

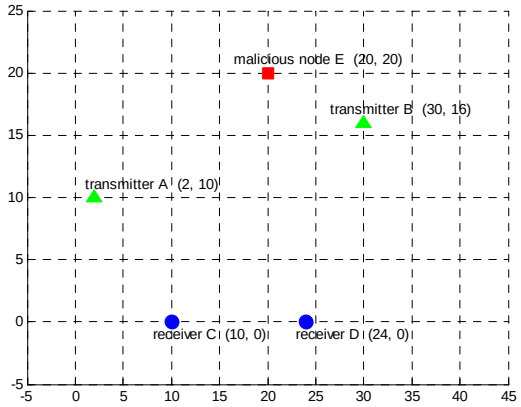

Figure 2. Deployment of sensor nodes for IRHF (the triangles and circles represent normal nodes of a ranging unit, and the rectangular represents malicious node).

First of all, we show that where the false estimation will locate through computer simulations, which will be compared with theoretical analysis in section III. Next the Monte Carlo simulations of the false-estimation probability will be presented in comparison with the closed-form expression in (32).

A. The Region of False Estimation

In the simulations, the carrier frequencies of the transmitted sine waves are chosen randomly within the band of W_{ss}=30 MHz, and the number of frequencies used in ranging is M=41 for each time. For simplicity, we assume SJRs at node C and D are with the same value of 0 dB, and the fraction of signals been jammed is $\beta = 0.5$. The range of parameter been searched is from -40 to 80.

Fig. 3 is the histogram for ML range estimators. The number of Monte Carlo Simulations is 10^4. It is clear that the majority of the estimates locate around two values, d_0 and d_0' . These estimation results locate not exactly but near d_0 and d_0' because of the random phase of $\phi_A - \phi_E$ in (18). This is the reason why the estimation appears like under the noise environment but the fact is that the simulations are without random noise.

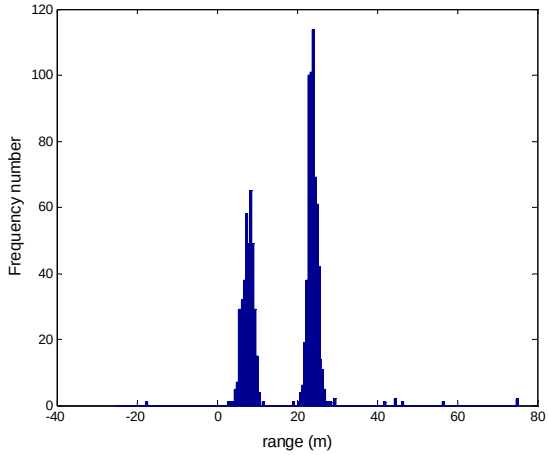

Figure 3. Histogram for ML range estimators of IRHF with B=30MHz and M=41.

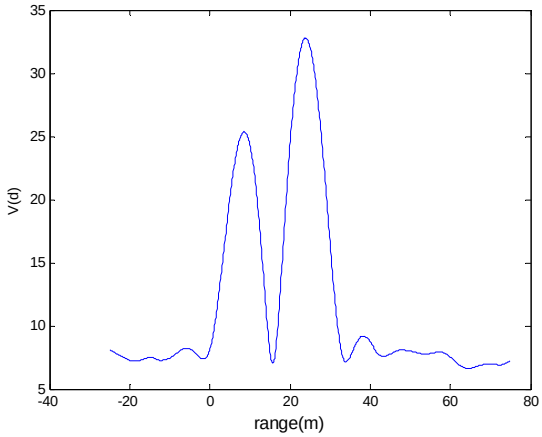

Figure 4. The average value of ML criterion function $V(d)$ of IRHF with B=30MHz and M=41.

Fig. 4 shows the average value of the criterion function (22) with respect to f_i. The specification of system parameters is as in Fig. 3. It is an important test because our analysis is based on this ML criterion function. From this figure we know that the average value of the criterion function has two peaks, one is at the true value d_0 , another is at the false one d_0'. Clearly, Fig. 4 coincides with the Fig.3, which verifies that our conclusion about the region of the false estimation in section Ⅲ is reasonable and valid.

B. The probability of False Estimation

In Fig.5, the probability of the false estimation is compared with the theoretical approximation (32). The value of W_{ss} and M are the same as before. Let the SJR at node C changes from -1 to 3 and its proportion to the SJR at node D is staying the same. This assumption is always valid due to two reasons. On the one hand, the relative positions of these nodes are fixed so the strength of signals will be constant at receivers. On the other hand, the jamming power at difference receivers will change with the same rate. What we have to control during the simulations is only that the difference of the SJR at two receivers is not remarkable.

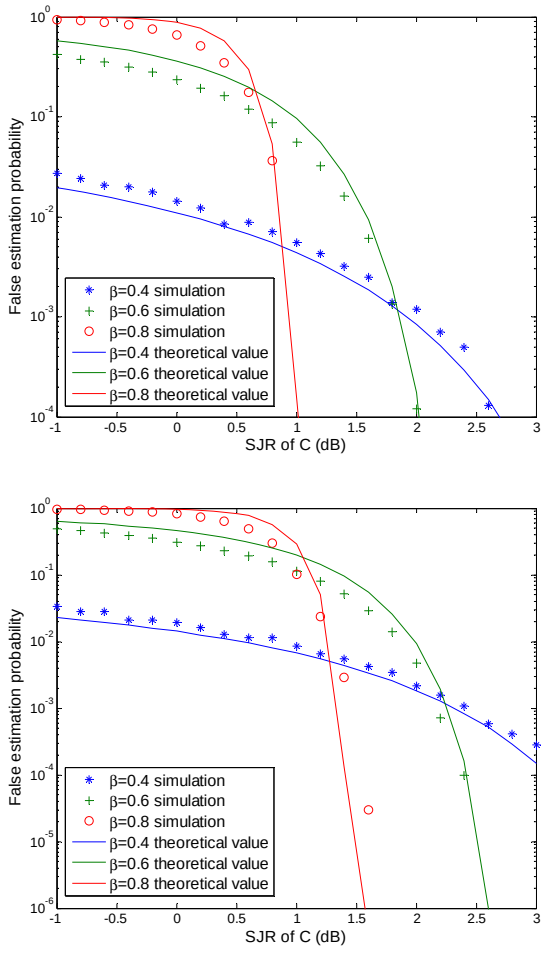

Figure 5. Monte Carlo simulations of the ML range estimator of IRHF under MTJ compared with theoretical approximations. (Top) The SJR ratio of C and D is 1:1. (Bottom) the SJR ratio at C and D is 1:1.2.

The simulations here will focus on two scenarios: in the top one of Fig. 5 we let $(S_c / I_c):(S_d / I_d)=1$, and in the bottom one of Fig. 5 we let $(S_c / I_c):(S_d / I_d)=1:1.2$. For each one, the values of the fraction of β are 0.4, 0.6 and 0.8. The number of Monte Carlo Simulations is 10^5 for each SJR. For concisely, we mark the horizontal axis by SJR of only node C.

From Fig.5 we find that the closed-form expression in (32) agrees well with the simulation results. If other system parameters are fixed, the probability of false estimation decreases as the SJR increases. When the SJR is fixed, the values of the false-estimation probability are also different with different values of the fraction β. The largest probability of false estimation corresponding to some certain fraction of β is called the 'worst-case jamming'. For different values of SJR, the fractions for the worst-case jamming are also different. It indicates that according to the theoretical results, one can modulate the system parameters to combat with the multi-tone jamming without time-consuming simulations.

V. CONCLUSION

This paper investigates the ranging performance of IRHF, an anti-jamming ranging technique for WSN, under multi-tone jammer. We detect that the main ill-effect caused by MTJ is the false estimation, and find that the exact value of the false estimation equals to the combination of one malicious node and the four ranging nodes. Furthermore, we have provided a closed-form expression of the false-estimation probability of ML estimator versus SJR and some system parameters. Simulation results agree well with the theoretical analysis. We conclude that the study results of this paper can predict the ML range estimator performance of IRHF precisely under multi-tone jammer.

To the best of our knowledge, it is the first time to evaluate the ranging performance of IRHF under MTJ, which provides a general framework to assess the performance of phase-based ranging technique under jamming environment. The computer simulation of false estimation is a long term operating. The theoretical approximation derived in this paper alleviates the need for time-consuming simulations.

ACKNOWLEDGMENT

This work has been supported in part by National Natural Science Foundation of China (No. 61273047 and 61301159) and the Natural Science Foundation of Jiangsu Province (No. BK20130068)

REFERENCES

[1] G. Mao, B. Fidan, and B. Anderson, "Wireless sensor network localization techniques", Computer networks, vol. 51, no. 10, pp.2529-2553, 2007.

[2] Z. Li, Y. Gu, L. Tang, H. Luo, G. Jin, "Fire hazard location algorithm for large place based on wireless sensor network", Journal of Computers, vol.9, no.3, pp. 711-716, 2014.

[3] T. Zhang, Y. Yin, D. Yue, X. Wang, G. Yu, "Research and implementation of an RFID simulation system supporting trajectory analysis", Journal of Software, vol.9, no.1, pp.162-168, 2014.

[4] M. Rudafshani, S. Datta, "Localization in wireless sensor networks", in proc. of the 6th International Symposium on Information Processing in Sensor Networks (IPSN). Cambridge, Massachusetts, USA, 2007.

[5] M. Maroti, B. Kusy, G. Balogh, P. Volgyesi, A. Nadas, K. Molnar, et al., "Radio interferometric geolocation", in proc. of the 3rd ACM International Conference on Embedded Networked Sensor Systems (SenSys), ACM, pp.1-12, November 2005.

[6] B. Kusy, A. Ledeczi, M. Maroti, L. Meertens, "Node density independent localization", in proc. Of the 5th International Symposium on Information Processing in Sensor Networks, ACM, pp.441-448, April 2006.

[7] B. Kusy, J. Sallai, G. Balogh, A. ledeczi, V. Protopopescu, J.Toliver, et al., "Radio interferometric tracking of mobile wireless nodes", in proc. of the 5th international conference on Mobile systems, applications and services. ACM, pp. 139-151, 2007.

[8] B. Kusy, A. Ledeczi and X. Koutsoukos, "Tracking mobile nodes using RF doppler shifts", in proc. Of the 5th international conference on Embedded Networked Sensor Systems (SenSys), ACM, pp. 29-42, 2007.

[9] Y. S. Zhu, P. Liu, S. Huang, "Parameter optimization method to extend deployment area of radio interferometric positioning system", Chinese Journal on Communications, vol. 31, no.9, pp.47-52, 2010.

[10] W. D. Qi, S. Zhang, Y. Zhang, J. B. Yang, "Radio interferometric positioning systems over wide scope", Journal of Huazhong University of Science and Technology (Natural Science Edition), vol.40, no.7, pp.95-99, 2012.

[11] C. Wang, Q. Y. Yin, W. J. Wang, "An efficient ranging method on Chinese remainder theorem for RIPS measurement", Science China Information Sciences, vol.53, no.6, pp.1233-1241, 2010.

[12] B. Xu, W.D. Qi, Y.S. Zhu, L. Wei. P. Liu, E. Yuan, "Frequency Selection in ECRT-based Radio Interferometric Ranging", Communications in Computer and Information Science, Springer, vol.334, pp.538-547, February 2013.

[13] A. Ledeczi, P. Volgyesi, J. Sallai, B. Kucy, "Towards precise indoor RF localization", in proc. of the 5th Workshop on Embedded Networked Sensors, Charlottesville: ACM, Jun, 2008.

[14] P. Liu, W. D. Qi, E. Yuan, Y. S. Zhu, H. Wang, "Ground displacement measurement by radio interferometric ranging for landslide early warning", in proc. of IEEE Instrum. and Meas. Technol. Conf. (I2MTC), pp.1-6, May 2011.

[15] Y. Wang, M. Shinotsuka, X. Ma, et al., "Design an asynchronous radio interferometric positioning system using dual-tone signaling", in Proc. of the Wireless Communications and Networking Conference (WCNC), IEEE, pp.2294–2298, 2013.

[16] W. C. Li, X. Z. Wang, W. Moran, "Distance estimation using wrapped phase measurements in noise", IEEE Trans. on Signal Processing, vol.61, no.7, pp.1676-1688, 2013.

[17] X. Z. Wang, B. Moran, M. Brazill, "Hyperbolic positioning using RIPS measurements for wireless sensor networks", in proc. of the 15th International Conference on

Networks (ICON). Adelaide, SA, Australia: IEEE, pp.425-430, 2007.
[18] S. Zhang, *Extended beat radio interferometry*, Nanjing: PLA University of science and technology, 2012.
[19] Y. Zhang, W. D. Qi, P. Liu, L. Wei, "Performance Analysis of Radio Interferometric Ranging", Chinese Journal of Scientific Instrument, vol. 35, no. 2, pp. 284-291, Feb. 2014.
[20] L. Wei, W. D. Qi, P. Liu, E. Yuan, Y. S. Zhu, X. J. Ji, "Method for selecting measurement frequencies based on dualp seudo-random code in Radio Interferometric Positioning System", Chinese Patent, CN102221695, 2013.
[21] I. Amundson, X. D. Koutsoukos, "A survey on localization for mobile wireless sensor networks", Mobile Entity Localization and Tracking in GPS-less Environnments. Springer Berlin Heidelberg, pp.235-254, 2009.
[22] P. Volgyesi, G. Balogh, A. Nadas, C. B. Nash, A ledeczi, "Shooter localization and weapon classification with soldier-wearable networked sensors", in proc. of the 5th international conference on Mobile systems, applications and services. ACM, pp.113-126, 2007.
[23] J. Sallai, P. Völgyesi, A. Lédeczi, K. Pence, T. Bapty, S. Neema, et al., "Acoustic shockwave-based bearing estimation", in proc. of the 12th international conference on Information processing in sensor networks, ACM, pp.217-228, 2013.
[24] F. Q. Yao, *Communication anti-jamming engineering and practice* (2nd Edition), Beijing: Publishing House of Electronics Industry, 2012.
[25] A.P. Richard. *Modern Communcation Jamming Principles and Techniques* (2nd Edition), Bosten: Artech Hourse, 2011.
[26] J. F. Jiang, G. J. Han, C. Zhu, Y. H. Dong, N. Zhang, "Secure localization in wireless sensor networks: A survey", Journal of Communications, vol.6, no.6, pp.460-470, 2011.
[27] Y. Zhang, W. D. Qi, W. H. Dai, J. Lv, G. X. Li, "The Performance of Interferometric Ranging Systems with Hopping Frequencies in Benign Environment and under Partial-Band Jamming", The 5th China Satellite Navigation Conference (CSNC), Nanjing, 2014.
[28] A. Papoulis, S. U. Pillai, *Probability, Random Variables and Stochastic Process* (4th edition), NewYork: McGraw-Hill Inc., pp.121, 2002.
[29] J. G. Proakis, *Digital Communications* (4th edition), Beijing: Publishing House of Electronics Industry, pp.943-948, 2006.
[30] S. F. Schnatter, *Finite Mixture and Markov Switching Models*, New York: Springer Science and Business Media, pp.10-11, 2006.

Yue Zhang received B.S. degree in 2009 from PLA University of Science and Technology on Network Engineering. She is currently pursuing the Ph.D. degree. Her current research interests include wireless sensor networks, Statistical signal processing, localization and navigation.

Wangdong Qi received B.S. degree from the Institute of Information Engineering in 1987, and the M.S. and Ph.D. degrees form the Institute of Communications Engineering in 1993 and 1997, respectively. He is currently a professor in PLA University of Science and Technology. His research interest is in wireless sensor networks, localization and network security.